



MK0500030

# Comparative Analysis of Nodal and Edge Finite Element Methods for Numerical Analysis of 3-D Magnetostatic Systems

Pavel MINTCHEV, Marin DIMITROV, and Stojimen BALINOV

*Institute of Metal Science - Bulgarian Academy of Sciences, 67 Shipchensky Prohod Str., 1574 Sofia, Bulgaria. Telephone: + 359 2 703 282, e-mail: balean@ims.bas.bg*

**Abstract.** The possibilities for applying the Finite Element Method (FEM) with gauged magnetic vector potential and the Edge Element Method (EEM) for three-dimensional numerical analysis of magnetostatic systems are analyzed. It is established that the EEM ensures sufficient accuracy for engineering calculations but in some cases its use results in bad convergence. The use of the FEM with gauged magnetic vector potential instead of the EEM is recommended for preliminary calculations of devices with complex geometry and large air gaps between the ferromagnetic parts.

## 1. Introduction

The calculation of the magnetic flux density in electrotechnological devices is an important stage in their design. The subject of the present work is three-dimensional numerical analysis of the magnetic field in magnetostatic electromagnetic systems. Both the Edge Element Method (EEM) [3] and the Finite Element Method (FEM) based on a system of differential equations for the magnetic vector potential (MVP) are applied. The Coulomb gauge is used for the FEM formulation [4].

In the case of the EEM the approximation of the magnetic field is done by circulation of the MVP along finite element edges. This ensures tangential continuity of the vector field and avoids the normal continuity. On the basis of this, high accuracy can be expected when calculating electromagnetic systems containing ferromagnetic details.

The application of the FEM with gauged MVP can result in errors when modeling systems containing ferromagnetic regions as a result of the violation of the continuity conditions on interfaces between ferromagnetic and non-ferromagnetic regions [5]. The advantage of this formulation is its good convergence [4].

The present paper examines the possibilities for applying both methods for numerical analysis of magnetostatic systems by comparing experimental data with the results of calculations of a device with complex geometry. The convergence of the numerical process when using both methods is also studied.

## 2. Formulation of the Problem

The following differential equation for the magnetic vector potential  $A$  is used in the case of the EEM:

$$\operatorname{rot}\left(\frac{1}{\mu}\operatorname{rot}A\right)=J, \quad (1)$$

where  $\mu$  is permeability and  $J$  is density of the exciting current.

After applying Galerkin's method and the EEM (1) is transformed into the functional:

$$\int_{\Omega}\left(\frac{1}{\mu}\operatorname{rot}A\right)(\operatorname{rot}W)d\Omega=\int_S W\times\left(\frac{1}{\mu}\operatorname{rot}A\right)dS-\int_{\Omega}J.Wd\Omega. \quad (2)$$

Here  $W$  is the weight function,  $\Omega$  is the region of integration and  $S$  is the boundary surface of  $\Omega$ .

The region of integration is discretized using tetrahedral finite elements. The weight function for an edge connecting the nodes with numbers  $i$  and  $j$  is defined as [1]:

$$W_e = \zeta_i \nabla \zeta_j - \zeta_j \nabla \zeta_i, \quad (3)$$

where  $\zeta$  is the shape function and  $e$  is the local number of the edge.

The following formulae are used to define  $A$ ,  $J$  and  $\operatorname{rot}A$  within a finite element [1,3]:

$$A = \sum_{e=1}^6 A_e W_e; \quad J = \sum_{e=1}^6 J_e W_e \quad (4)$$

$$\operatorname{rot}A = \sum_{e=1}^6 A_e \operatorname{rot}W_e; \quad \operatorname{rot}W_e = 2\nabla\zeta_i \times \nabla\zeta_j \quad (5)$$

Here  $A_e$  and  $J_e$  are circulations of  $A$  and  $J$  along a finite element edge.

Applying (2), (3), (4) and (5) for each of the edges of the net of finite elements results in a system of algebraic equations.

An algorithm based on the following differential equation for the MVP

$$\operatorname{rot}\left(\frac{1}{\mu}\operatorname{rot}A\right)-\operatorname{grad}\left(\frac{1}{\mu}\operatorname{div}A\right)=J \quad (6)$$

is used for the FEM numerical calculations [4]. Equation (6) includes the Coulomb gauge  $\operatorname{div}A = 0$  [4].

After applying Galerkin's method and the FEM (6) is transformed into a system of algebraic equations.

The Incomplete Cholesky-Conjugate Gradient (ICCG) Method [6] is used to solve the systems of algebraic equations. The accuracy of the solution of the system is evaluated by means of the relative Euclidean norm of the residuals  $e_i$  [4].

### 3. Numerical Algorithms

A numerical algorithm with two iteration cycles is usually applied for the EEM and FEM. The first cycle includes solving the systems of algebraic equations and determining the values of the magnetic flux density for each element. Each iteration of the second cycle includes the whole first cycle as well as corrections of the current values of the permeabilities for the elements with non-linear properties according to the magnetic characteristics of the materials.

The use of this algorithm for the FEM does not create problems. However, its application for the EEM in the case of magnetic systems with complex geometry results in a rather long computation time. A second algorithm was created in order to solve this problem. It is applicable for EEM modeling of devices in which a part of the magnetic system is not saturated [7]. According to the algorithm, the calculations are divided into two stages. During the first stage the number of the elements is reduced by simplifying the construction of the non-saturated part. The two iteration cycles are then implemented. The calculated values of the permeabilities for the finite elements of the saturated part are used during the second stage to calculate the distribution of the magnetic flux density in the real system by implementing only the first iteration cycle.

### 4. Experimental and Theoretical Results

An experimental and theoretical study of the electromagnetic system of a device for the bonding of steel tubes by means of a magnetically driven arc (Fig.1) [8] is implemented in order to compare the two methods.

The magnetic cores and the bonded tubes are made of steel. The two coils contain 3,540 turns, have different polarities and are connected to a DC supply voltage. It is assumed that the exciting current is distributed in prismatic regions with cross-section equal to that of the coils. In the figure the region of integration, which includes 1/8 of the volume of the device, is hatched.

The condition

$$\mathbf{B} \cdot \mathbf{n} = 0, \quad (7)$$

where  $\mathbf{n}$  is the outer normal to the surface is imposed on all boundary surfaces. It is transformed into the following equations for the MVP:

$$\mathbf{A} \times \mathbf{n} = 0 \quad (8)$$

for the FEM and

$$\mathbf{A}_e = 0 \quad (9)$$

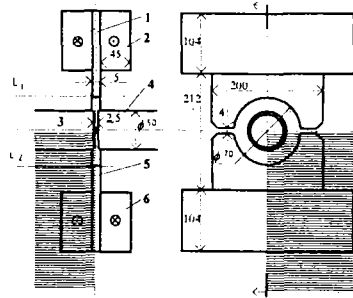
for the EEM.

Calculations for the distribution of the magnetic flux density at three values of the exciting current: 1, 3.5 and 7A are made by computer programs implementing both algorithms. In the case of the FEM the region of integration is divided into 756

hexahedral elements. The net for the EEM is obtained by dividing each hexahedral element into 6 tetrahedral ones.

It was established by means of preliminary numerical experiments that the

**Fig. 1. Electromagnetic system of a device for bonding of steel tubes by means of a magnetically driven arc. 1, 5 – magnetic cores; 2, 6 – coils (number of turns  $w=3,640$ ); 3, 4 – bonded tubs. All dimensions are in mm.**



ferromagnetic regions situated between the planes  $L_1$  and  $L_2$  (Fig. 1) are not saturated even for the highest value of the exciting current. The plane  $L_2$  is defined as a boundary between the saturated and the non-saturated parts of the region of integration. During the first stage of the calculations by the EEM, the construction of the non-saturated part is simplified by ignoring the tubes pos. 3 and 4 and replacing the magnetic cores pos. 1 and 5 with a metal plate. It is established that this simplification has practically no influence on the magnetic flux density in the ferromagnetic elements of the saturated part of the device.

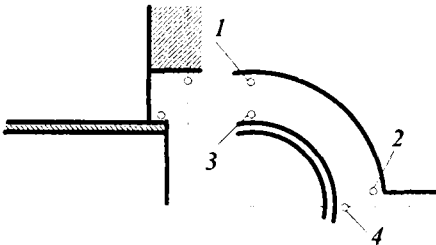


**Fig. 2. Location of the control points.**

located according to Fig. 2. The distance from each point to the nearest metal surface is approximately 1.5 mm.

**Table I. Experimental values of  $B_r$ , T**

|          | I, A | 1     | 3.5   | 7     |
|----------|------|-------|-------|-------|
| Point No | 1    | 0.085 | 0.270 | 0.405 |
|          | 2    | 0.082 | 0.255 | 0.390 |
|          | 3    | 0.055 | 0.190 | 0.280 |
|          | 4    | 0.060 | 0.175 | 0.270 |

The FEM calculations are performed according to the first algorithm.

The following results can be used to evaluate the convergence of both methods: to solve with  $e_i < 0.04$  the systems of algebraic equations compiled after discretizing the original electromagnetic system, 15,000 ICCG iterations are needed for the EEM and 1,120 for the FEM. In both cases the initial values of the unknowns are zero.

The radial (in relation to the bonded tubes) components  $B_r$  of the magnetic flux density are measured in four control points

In Table 1 are shown the measured values of  $B_r$  in the four control points according to Fig. 2. In Tables 2 and 3 are given the results of the calculations obtained by the EEM and the FEM, as well as the relative differences  $\Delta$  between the theoretical and the experimental results. The

maximum absolute value of  $\Delta$  for the EEM is 12.7% while for the FEM with gauged MVP it is 23.1%. The average absolute value of  $\Delta$  is 6.2% for the EEM and 11.4% for the FEM.

Table II. Results of the calculation of  $B_r$  by the EEM and relative difference  $\Delta$  between the calculated and the experimental data

| I, A     | 1        |              | 3.5      |              | 7        |              |
|----------|----------|--------------|----------|--------------|----------|--------------|
| Point No | $B_r, T$ | $\Delta, \%$ | $B_r, T$ | $\Delta, \%$ | $B_r, T$ | $\Delta, \%$ |
| 1        | 0.095    | 11.7         | 0.279    | 3.3          | 0.421    | 3.9          |
| 2        | 0.088    | 7.3          | 0.273    | 7.0          | 0.399    | 2.3          |
| 3        | 0.062    | 12.7         | 0.184    | -3.1         | 0.286    | 2.1          |
| 4        | 0.063    | 5.0          | 0.190    | 8.6          | 0.289    | 7.0          |

Table III. Results of the calculation of  $B_r$  by the FEM and relative difference  $\Delta$  between the calculated and the experimental data

| I, A     | 1        |              | 3.5      |              | 7        |              |
|----------|----------|--------------|----------|--------------|----------|--------------|
| Point No | $B_r, T$ | $\Delta, \%$ | $B_r, T$ | $\Delta, \%$ | $B_r, T$ | $\Delta, \%$ |
| 1        | 0.087    | 2.8          | 0.227    | -15.9        | 0.319    | -21.2        |
| 2        | 0.067    | -18.0        | 0.217    | -14.9        | 0.300    | -23.1        |
| 3        | 0.066    | 19.4         | 0.185    | -2.6         | 0.278    | -0.7         |
| 4        | 0.065    | 8.8          | 0.188    | 7.4          | 0.275    | 1.8          |

## 5. Conclusions

A magnetostatic system with complex geometry and large air gaps between the ferromagnetic parts has been numerically modeled by means of different formulations of the Finite Element Method. The numerical results have been verified experimentally. The following conclusions can be drawn from the investigation:

- the use of Edge Element Method in the modeling of the investigated systems ensures accuracy sufficient for engineering calculations, but problems may occur as a result of bad convergence.

- the use of the Finite Element Method with gauged magnetic vector potential is recommended for the preliminary calculations of the investigated systems because of its fast convergence.

## References

- [1] A. Bossavit, "Whitney Forms: a Class of Finite Elements for Three- Dimensional Computations in Electromagnetism," *IEE Proc. A*, vol. 135, no 8, pp. 493-500, 1988.
- [2] K. Preis, I. Bardi, O. Biro, C. Magele, G. Vrisk, and R. Richter, "Different Finite Element Formulation of 3D Magnetostatic Fields," *IEEE Trans. on Magn.*, vol. 28, no 2, pp. 1056-1059, March 1992.
- [3] N. Goliás and T. Tsiboukis, "3-D Eddy-Current Computation with a Self-Adaptive Refinement Technique," *IEEE Trans. on Magn.*, vol. 31, no 3, pp. 2261-2268, 1995.
- [4] O. Biro and K. Preis, "On the Use of the Magnetic Vector Potential in the Finite Element Analysis of the Three-Dimensional Eddy Currents," *IEEE Trans. on Magn.*, vol. 25, no 4, pp. 3145-3159, July 1989.
- [5] Mimoun S.M., J.Fouladgar and G.Develey. "Modeling of 3D Electromagnetic and Heat Transfer Phenomena for Materials with Poor Conductivity". *IEEE Trans. on Magn.*, pp. 3578-3580, November 1995.
- [6] Kershaw D, "The Incomplete Cholesky-Conjugate Gradient Method for the Iterative Solution of Systems of Linear Equations," *Journal of Computational Physics*, no 26, pp.43-65, 1978.
- [7] M. Dimitrov and P. Mintchev, "Three Dimensional Numerical Analysis of Magnetostatic Systems," *Technical Ideas*, No 3-4, pp. 34-39, 1998 (in Bulgarian).
- [8] K Mazac, "Spulensysteme für das Schweissen mit Magnetisch Bewegtem Lichtbogen," *Schweissen und Schneiden*, no 4, 1984.